

Electrically Poled Vapor-Deposited Organic Glasses for Integrated Electro-Optics

LAUREN DALLACHIESA,¹ AND IVAN BIAGGIO^{1,*}

¹Department of Physics and Center for Photonics and Nanoelectronics, Lehigh University, Bethlehem, PA 18015

*Corresponding author: biaggio@lehigh.edu

Compiled May 21, 2024

We introduce electrically-poled small molecule assemblies that can serve as the active electro-optic material in nano-scale guided-wave circuits such as those of the silicon photonics platform. These monolithic organic materials can be vacuum-deposited to homogeneously fill nanometer-size integrated-optics structures, and electrically poled at higher temperatures to impart an orientational non-centrosymmetric order that remains stable at room temperature. An initial demonstration using the DDMEBT molecule and corona poling delivered a material with the required high optical quality, an effective glass transition temperature of the order of $\sim 80^\circ\text{C}$, and an electro-optic coefficient of 20 pm/V . © 2024 Optical Society of America

<http://dx.doi.org/10.1364/ao.XX.XXXXXX>

Conjugated organic molecules, when combined into a material compatible with integrated optics, can contribute strong and fast nonlinear optical functionalities to state-of-the-art integrated photonics platforms that already provide unprecedented control of optical modes and their propagation. Silicon-organic-hybrid electro-optic modulators have already been demonstrated on the silicon photonics platform [1–3] using electrically poled polymers [4–7]. These organic materials enable ultrafast electro-optic modulation because of their low dielectric constant and ultrafast electronic response of conjugated molecules.

However, even though electrically poled polymers have been developed over many decades and have record-high electro-optic coefficients [7–10], they are deposited from solution in a wet process that poses challenges towards a reproducible homogenous filling of nanostructures, especially when working with nanoscale gaps of the order of $\sim 100\text{ nm}$ or less [6]. It is therefore important to investigate alternatives to polymers for the integration of organic materials and their active functionality into future photonics circuitry.

Here we propose vapor deposition of small molecules and subsequent electric poling of the resulting monolithic molecular assembly. Vacuum thermal evaporation of small organic molecules is currently widely used in the industrial production of organic light emitting displays [11]. This dry, solvent-free process would enable the homogenous filling of nanoscale integrated optical elements such as slot waveguides, photonic

bandgap structures, or subwavelength waveguides [3, 12–14], and also offers a nanometer-level control of thickness and precise mask-defined deposition areas.

The electrically-poled small molecule assemblies (PSMA) discussed in this work are monolithic, dense organic materials consisting of small dipolar molecules, and fulfill the following requirements: (1) the molecules sublime without decomposition, enabling the use of vacuum thermal evaporation in manufacturing; (2) the material obtained after deposition on any substrate is homogenous with a high optical quality; and (3) the material can be electrically poled at higher temperatures to impart a stable electro-optic activity. In these systems [15], a higher molecular number density will at least partially compensate the necessarily lower optical nonlinearity of smaller molecules.

As a background, we note that some non-lattice-matched deposition of small-molecule assemblies with orientational order has been demonstrated earlier, but did not generally involve molecules with large dipole moments or deliver electro-optic activity [16–20], or else relied on directional hydrogen-bonding sites that required specially prepared substrates [21]. Vapor-transport deposition of crystalline films has also been experimented with [22–24], but cannot be readily adapted to growing a single crystal over millimeter distances inside nano-scale structures.

For this demonstration, we used a material (DDMEBT [25], see Fig. 1) that already fulfills requirements (1) and (2) in the above list: it deposits well using vacuum thermal evaporation [25] and leads to a high optical-quality, homogenous material [15, 25–27]. In this work, we show that it also fulfills requirement (3). DDMEBT is a compact donor-acceptor substituted molecule with a high specific third-order polarizability [28], and it has already been shown to homogeneously fill the gap of a slot waveguide used for all-optical switching [26, 27]. This molecule is also interesting for a PSMA because it has a dipole moment of 11 Debye [29], and a second order nonlinear optical polarizability estimated to be of the order of $35 \times 10^{-39}\text{ m}^4/\text{V}$ [30].

We deposited the DDMEBT material on glass substrates coated with Indium Tin Oxide (ITO) using vacuum molecular beam deposition at a pressure of 10^{-5} Torr, with a deposition rate of $\sim 1\text{ nm/min}$. Films with thicknesses ranging from 100 nm to 750 nm were then poled by applying an electric field at higher temperatures using corona poling [32, 33]. The second order nonlinear optical susceptibility of the films, which directly relates to the degree of orientational ordering, was determined

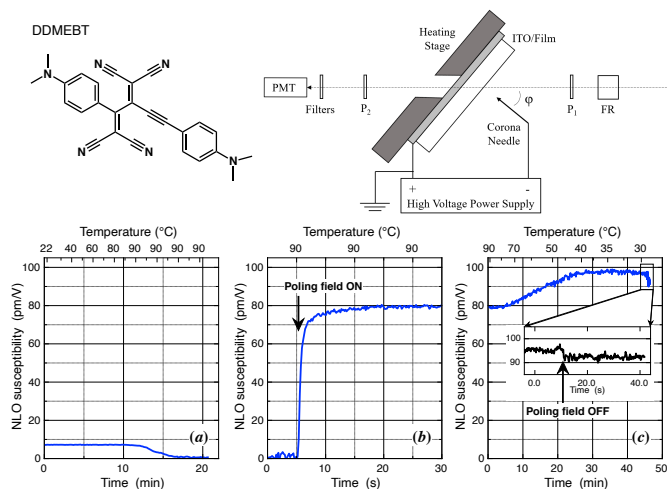


Fig. 1. Top: The DDMEBT molecule, with chemical formula $C_{26}H_{20}N_6$, and full name [2-[4-(Dimethylamino)phenyl]-3-([4(dimethylamino)phenyl]- ethynyl)-buta-1,3-diene-1,4,4-tetracarbonitrile] [25, 31], and a scheme of the corona poling apparatus used in this work. Bottom: Poling procedure performed with a poling voltage of 5.5 kV on a 250 nm thick DDMEBT film. The plots give the second order nonlinear optical susceptibility of the film observed during the experiment. The bottom horizontal axis in every plot is time (note the different scale of the middle plot and the inset in the third plot). The tic marks on the top horizontal axes of every plot give the sample temperature at the corresponding moment in time.

using second harmonic generation (SHG) before, during, and after corona poling.

For our SHG experiments we used 1 ps duration laser pulses at an off-resonant wavelength of 1500 nm and a repetition rate of 1 kHz, produced by a TOPAS (Traveling Wave Optical Parametric Amplifier System) from Light Conversion, pumped by a Clark MXR Ti:Sapphire amplifier (CPA-2001). The sample was mounted on a rotation stage, and its second-order nonlinear optical susceptibility was obtained by comparing, in a Maker fringes experiment [34, 35], the incidence-angle dependence of the SHG signal of the organic films to that of a 2 mm thick quartz crystal (nonlinear optical susceptibility of $\chi_{111}^{(2)} = 0.6$ pm/V, corresponding to a “d-coefficient” $d_{111} = 0.3$ pm/V [36]).

SHG characterization at room temperature showed that as grown DDMEBT films already have a slight preferential molecular orientation that breaks symmetry in a direction perpendicular to the substrate and induces a small second-order nonlinear optical susceptibility [37]. This is a characteristic of some vapor deposited organic glasses [18–20, 38–41], where an orientational order arises from the assembly process of the molecules at the vacuum-film interface [18, 40]. Our thickness-dependent SHG measurements imply that this orientational order is built into the DDMEBT film throughout its whole thickness.

Electrical poling was done in a corona poling set-up (see Fig. 1) with in-situ SHG characterization. Fig. 1 shows plots of the second-order susceptibility of the organic film, as it is continually observed during the whole procedure. Fig. 1(a) is for the initial heating of the film between room temperature and 90°C, using a linear ramp of 5°C per minute. The second order susceptibility already observed at room temperature is the intrinsic one imposed during vacuum deposition. It then starts

slowly decreasing above 70°C as the intrinsic orientational order is being thermally randomized, and vanishes completely after a few minutes at 90°C (see Fig. 1a). This behavior is characteristic of an effective glass-transition temperature, an interpretation supported by the fact that the as-grown material is an amorphous molecular assembly with properties similar to previously investigated vapor-deposited organic glasses [19, 20, 38–41].

Once the intrinsic preferential orientational order completely disappeared at 90°C, a voltage of 5.5 kV was applied to the corona needle. This caused the second-order susceptibility (Fig. 1b) to rise to a value of $\chi^{(2)} \sim 80$ pm/V within a fraction of a second. The film is then cooled back down while keeping the applied electric field constant (Fig. 1c). Interestingly, during the slow cooling process (about 40 minutes to reach 30°C), the second-order susceptibility, and therefore the orientational order, continued to increase, to then reach a final value of ~ 100 pm/V that remained stable at room temperature.

Switching off the corona poling voltage at this point only caused a small drop in second-order susceptibility, consistent with the third-order nonlinear optical process of electric-field-induced SHG, as described by

$$\frac{SHG(E = E_c)}{SHG(E = 0)} = \left[1 + \frac{\chi_{111}^{(2)}}{\chi_{1111}^{(3)} E_c} \right]^2, \quad (1)$$

where E_c is the effective electric field inside the material, the left-hand side is the ratio between the SHG powers measured with and without the corona poling voltage, $\chi_{1111}^{(3)} = (2 \pm 1) \times 10^{-19} \text{ m}^2\text{V}^{-2}$ is the third-order susceptibility of DDMEBT at a wavelength of 1.5 μm [25, 42], and $\chi_{111}^{(2)}$ is the second order susceptibility determined in this work. From this we can estimate the actual electric field that is present inside the film in our experiments to be of the order of $E_c = 50 \text{ kV/mm} = 50 \text{ V}/\mu\text{m}$ with an uncertainty of $\pm 50\%$.

The continued increase of the preferential orientational order when the films are cooled under the applied electric field is not generally observed when similar procedures are applied to molecules in a solid solution such as a polymer-based guest-host systems. However, our material is made up of a dense monolithic assembly of small molecules. Therefore, the molecular dipoles cannot simply reorient, there also needs to be a rearrangement of the molecular packing, which in this case appears to continue to occur, slowly, at lower temperatures. While more experiments will be needed to completely characterize this process, we can tentatively speculate that the DDMEBT molecular structure may play a role. This molecule consists of two parts that are almost perpendicular to each other. The corresponding rotation angle around the single bond is of 96.7 degrees [43], close to perpendicular. This may give this molecule some flexibility in adapting to its environment upon thermal perturbations. This very flexibility likely aids towards forming an amorphous solid state upon deposition, and it is reasonable to assume that it also plays a role in the continued growth of the orientational order of the DDMEBT solid state material that is observed (see Fig. 1c) at temperatures slightly below the poling temperature.

We repeated the experiment several times and confirmed that the poling procedure described above also works at slightly lower or larger poling temperatures, with longer times for the randomization of the intrinsic order at the lower temperatures, a sub-second build-up of the electric-field-induced ordering when applying the corona voltage, and an additional slower

improvement of the order later on. Poling results in different samples are given in Table 1. The sample-to-sample variations in the electro-optic coefficient shown in this table are generally small, and they could also be attributed to slight changes in the corona poling setup (such as the type of needle or the gap between the tip of the needle and the film). The one outlier with the significantly lower value belongs to an earlier experiment.

We have not seen any detrimental effects of the poling procedure on the vapor-deposited material, which remains of high optical quality, with no signs of crystallization (as confirmed by light scattering and x-ray diffraction). In addition to this, SHG characterization was repeated at different times after deposition (up to a year), and confirmed that the preferential molecular orientation remains stable. The results of a full Maker fringes SHG measurement of three poled films with different thicknesses and of the quartz reference is shown in Fig. 2. The second-order nonlinear optical susceptibility of the poled films was obtained by comparing the SHG power from the films and from the quartz reference while taking into account all projections of the optical fields, Fresnel transmission coefficients, and the DDMEBT refractive indices of 1.8 at 1550 nm and 2.0 at 750 nm (see Ref. [25] for the refractive index dispersion in DDMEBT). The result obtained from the data in Fig. 2 is $\chi_{111}^{(2)} = 100 \pm 30$ pm/V for all three films with different thicknesses, showing that the orientational order is maintained throughout the bulk of the material and is reproducible between different samples.

In organic materials, one expects a good correspondence between the susceptibilities for SHG and for electro-optics, leading to the following relationship between the second-order susceptibility for SHG and the standard electro-optic coefficient r_{ijk} ,

$$\chi_{ijk}^{(2)}(-\omega, \omega, 0) = -\frac{1}{2} n_i^2 n_j^2 r_{ijk}, \quad (2)$$

where $n_1 = n_2 = n_3 = 1.8$ is the refractive index of the DDMEBT material at $1.5 \mu\text{m}$ [25]. Here we can use the isotropic refractive index determined for the as-grown material because the preferential (incomplete) alignment that we obtain after poling has a negligible influence on the linear optical properties. Applying this expression to the experimental value of $\chi^{(2)} = 100 \pm 30$ pm/V we find that the corresponding electro-optic coefficient for a pure electronic response and ultra-fast electro-optic modulation is $r_{111} = 20$ pm/V. As a reference, this value is only $\sim 30\%$ lower than the electro-optic coefficients of standard electro-optic crystals such as ferroelectric KTP (KTiOPO_4) or LiNbO_3 .

Table 1. Electro-optic coefficients obtained in DDMEBT films after applying the high-temperature corona poling procedure shown in Fig. 1 (from SHG characterization and Eq.2).

Film Thickness (nm)	Corona Voltage (kV)	r_{111} (pm/V)
250	-5.5	20
300	-5.0	13
350	-5.0	18
420	-5.5	22
750	-5.5	18

The size of the electro-optic coefficient of the PSMA demon-

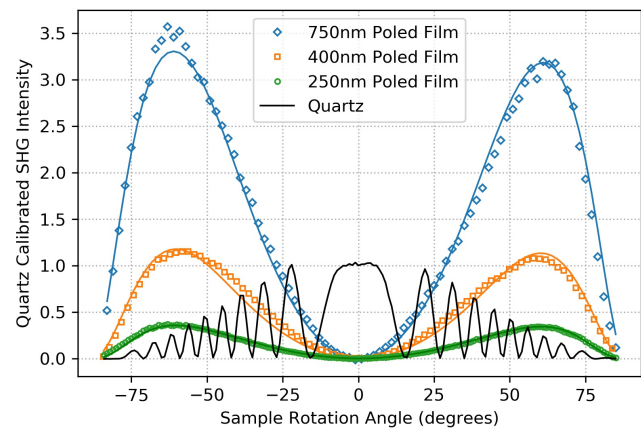


Fig. 2. Incidence angle dependence of SHG from three different PSMA films and the quartz reference. Both fundamental and second-harmonic are polarized parallel to the incidence plane. The solid curves are theoretical fits with a second-order susceptibility for the films of $\chi_{111}^{(2)} = 100$ pm/V, where the 1-axis is perpendicular to the substrate

strated here could already enable a ultra-high-speed electro-optic modulator on the silicon photonics platform using a millimeter-long slot-waveguide [44]. Still, we should point out that in our experiments the poling electric field was limited to an estimated $50 \text{ kV/mm} = 50 \text{ V}/\mu\text{m}$, but the use of up to five times higher poling electric fields is possible [4, 5, 7]. In addition, this PSMA value of $r_{111} = 20$ pm/V was obtained using an off-the-shelf molecule that was not explicitly optimized for electro-optics or for this fabrication method. There is therefore still a strong potential for future improvements.

In conclusion, the present demonstration of an electrically poled monolithic small-molecule assembly shows that the necessarily weaker second-order polarizability of a small molecule that can sublime without decomposition can be compensated by the larger molecular number-density in a monolithic PSMA. An electro-optic coefficient of 20 pm/V was demonstrated, and there is potential for significant improvements after research on the optimization of molecular structure and properties.

The ability to integrate the organic material with existing state-of-the-art guided-wave technology using vacuum thermal evaporation instead of a wet process of deposition from solution enables a better control of the deposition process and homogeneous incorporation of the organic material using a technique that can be easily scaled from the laboratory to industrial production [11].

PSMAs can therefore become a valuable alternative paradigm towards adding a second-order nonlinear optical functionality to integrated optics platforms, not only for electro-optic effects, but also for such applications as optical parametric generators or single photon or photon-pair sources.

Disclosures. The authors declare no conflicts of interest.

REFERENCES

- J. Leuthold, W. Freude, J. M. Brosi, R. Baets, P. Dumon, I. Biaggio, M. L. Scimeca, F. Diederich, B. Frank, and C. Koos, Proc. IEEE **97**, 1304 (2009).
- D. Thomson, A. Zilkie, J. E. Bowers, T. Komljenovic, G. T. Reed, L. Vivien, D. Marris-Morini, E. Cassan, L. Viroat, J.-M. Fédéli, J.-M. Hart-

- mann, J. H. Schmid, D.-X. Xu, F. Boeuf, P. O'Brien, G. Z. Mashanovich, and M. Nedeljkovic, *J. Opt.* **18**, 073003 (2016).
3. P. Cheben, R. Halir, J. H. Schmid, H. A. Atwater, and D. R. Smith, *Nature* **560**, 565 (2018).
 4. R. Palmer, S. Koeber, D. L. Elder, M. Woessner, W. Heni, D. Korn, M. Lauermann, W. Bogaerts, L. Dalton, W. Freude, J. Leuthold, and C. Koos, *J. Light. Technol.* **32**, 2726 (2014).
 5. M. Lauermann, C. Weimann, A. Knopf, W. Heni, R. Palmer, S. Koeber, D. L. Elder, W. Bogaerts, J. Leuthold, L. R. Dalton, C. Rembe, W. Freude, and C. Koos, *Opt. Express* **24**, 11694 (2016).
 6. W. Heni, C. Haffner, D. L. Elder, A. F. Tillack, Y. Fedoryshyn, R. Cottier, Y. Salamin, C. Hoessbacher, U. Koch, B. Cheng, B. Robinson, L. R. Dalton, and J. Leuthold, *Opt. Express* **25**, 2627 (2017).
 7. C. Kieninger, Y. Kutuvantavida, D. L. Elder, S. Wolf, H. Zwickel, M. Blaicher, J. N. Kemal, M. Lauermann, S. Randel, W. Freude, L. R. Dalton, and C. Koos, *Optica* **5**, 739 (2018). Publisher: Optical Society of America.
 8. L. R. Dalton, *J. Physics: Condens. Matter* **15**, R897 (2003).
 9. L. R. Dalton, P. A. Sullivan, and D. H. Bale, *Chem. Rev.* **110**, 25 (2010).
 10. L. Dalton and S. Benight, *Polymers* **3**, 1325 (2011).
 11. J. P. Spindler, J. W. Hamer, and M. E. Kondakova, "Oled manufacturing equipment and methods," in *Handbook of Advanced Lighting Technology*, R. Karlicek, C.-C. Sun, G. Zissis, and R. Ma, eds. (Springer International Publishing, Cham, 2017), pp. 417–441.
 12. Z. Pan, X. Xu, C.-J. Chung, H. Dalir, H. Yan, K. Chen, Y. Wang, B. Jia, and R. T. Chen, *Laser & Photonics Rev.* **12**, 1700300 (2018).
 13. A. Govdeli, M. C. Sarihan, U. Karaca, and S. Kocaman, *Sci. Reports* **8**, 1619 (2018).
 14. R. R. Ghosh, P. Bhardwaj, N. Gupta, S. Subramanian, and A. Dhawan, "Broadband electro-optic modulator based on a phase-change material embedded in silicon photonic crystal slab waveguide," in *Silicon Photonics XIV*, vol. 10923 G. T. Reed and A. P. Knights, eds., International Society for Optics and Photonics (SPIE, 2019), pp. 214 – 221.
 15. I. Biaggio, *Chem. – A Eur. J.* **28**, e202103168 (2022).
 16. D. Yokoyama, A. Sakaguchi, M. Suzuki, and C. Adachi, *Appl. Phys. Lett.* **95**, 243303 (2009).
 17. D. Yokoyama, Y. Setoguchi, A. Sakaguchi, M. Suzuki, and C. Adachi, *Adv. Funct. Mater.* **20**, 386 (2010).
 18. L. Zhu, C. W. Brian, S. F. Swallen, P. T. Straus, M. D. Ediger, and L. Yu, *Phys. Rev. Lett.* **106**, 256103 (2011). Publisher: American Physical Society.
 19. K. J. Dawson, L. Zhu, L. Yu, and M. D. Ediger, *The J. Phys. Chem. B* **115**, 455 (2011). Publisher: American Chemical Society.
 20. M. D. Ediger, J. de Pablo, and L. Yu, *Accounts Chem. Res.* **52**, 407 (2019). Publisher: American Chemical Society.
 21. C. Cai, M. M. Bösch, B. Müller, Y. Tao, A. Kündig, C. Bosshard, Z. Gan, I. Biaggio, I. Liakatas, M. Jäger *et al.*, *Adv. Mater.* **11**, 745 (1999).
 22. P. E. Burrows, S. R. Forrest, L. S. Sapochak, J. Schwartz, P. Fenter, T. Buma, V. S. Ban, and J. L. Forrest, *J. Cryst. Growth* **156**, 91 (1995).
 23. S. R. Forrest, P. E. Burrows, A. Stroustrup, D. Strickland, and V. S. Ban, *Appl. Phys. Lett.* **68**, 1326 (1996). Publisher: American Institute of Physics.
 24. M. Baldo, M. Deutsch, P. Burrows, H. Gossenberger, M. Gerstenberg, V. Ban, and S. Forrest, *Adv. Mater.* **10**, 1505 (1998).
 25. B. Esembeson, M. L. Scimeca, I. Biaggio, T. Michinobu, and F. Diederich, *Adv. Mater.* **19**, 4584 (2008).
 26. C. Koos, P. Vorreau, T. Vallaitis, P. Dumon, W. Bogaerts, R. Baets, B. Esembeson, I. Biaggio, T. Michinobu, F. Diederich, W. Freude, and J. Leuthold, *Nat. Photonics* **3**, 216 (2009). Number: 4 Publisher: Nature Publishing Group.
 27. M. Scimeca, I. Biaggio, B. Breiten, F. Diederich, T. Vallaitis, W. Freude, and J. Leuthold, *Opt. Photonics News* **20**, 39 (2009). Publisher: Optical Society of America.
 28. M. A. Erickson, M. T. Beels, and I. Biaggio, *J. Opt. Soc. Am. B* **33**, E130 (2016).
 29. F. Bureš, O. Pytela, M. Kivala, and F. Diederich, *J. Phys. Org. Chem.* **24**, 274 (2011). [_eprint: https://onlinelibrary.wiley.com/doi/pdf/10.1002/poc.1744](https://onlinelibrary.wiley.com/doi/pdf/10.1002/poc.1744).
 30. L. Dallachiesa, "Vapor Deposited Organic Glasses for Integrated Electro-Optics," Ph.D. thesis, Lehigh University (2021).
 31. T. Michinobu, C. Boudon, J.-P. Gisselbrecht, P. Seiler, B. Frank, N. N. P. Moonen, M. Gross, and F. Diederich, *Chem. Eur. J.* **12**, 1889 (2005).
 32. J. Giacometti and O. Oliveira, *IEEE Transactions on Electr. Insulation* **27**, 924 (1992). Conference Name: IEEE Transactions on Electrical Insulation.
 33. M. Eich, A. Sen, H. Looser, G. C. Bjorklund, J. D. Swalen, R. Twieg, and D. Y. Yoon, *J. Appl. Phys.* **66**, 2559 (1989). Publisher: American Institute of Physics.
 34. J. Jerphagnon and S. K. Kurtz, *J. Appl. Phys.* **41**, 1667 (1970).
 35. W. N. Herman and L. M. Hayden, *J. Opt. Soc. Am. B* **12**, 416 (1995).
 36. R. Eckardt, H. Masuda, Y. Fan, and R. Byer, *IEEE J. Quantum Electron.* **26**, 922 (1990).
 37. M. A. Erickson, "In-situ Poling of Organic Supramolecular Assemblies for Integrated Nonlinear Optics," Ph.D. thesis, Lehigh University (2018).
 38. H.-W. Lin, C.-L. Lin, H.-H. Chang, Y.-T. Lin, C.-C. Wu, Y.-M. Chen, R.-T. Chen, Y.-Y. Chien, and K.-T. Wong, *J. Appl. Phys.* **95**, 881 (2004). Publisher: American Institute of Physics.
 39. K. Dawson, L. A. Kopff, L. Zhu, R. J. McMahon, L. Yu, R. Richert, and M. D. Ediger, *The J. Chem. Phys.* **136**, 094505 (2012).
 40. I. Lyubimov, L. Antony, D. M. Walters, D. Rodney, M. D. Ediger, and J. J. de Pablo, *The J. Chem. Phys.* **143**, 094502 (2015).
 41. M. D. Ediger, *Proc. Natl. Acad. Sci.* **111**, 11232 (2014). Publisher: National Academy of Sciences Section: Commentary.
 42. M. T. Beels, M. S. Fleischman, I. Biaggio, B. Breiten, M. Jordan, and F. Diederich, *Opt. Mater. Express* **2**, 294 (2012).
 43. T. Michinobu, C. Boudon, J.-P. Gisselbrecht, P. Seiler, B. Frank, N. Moonen, M. Gross, and F. Diederich, *Chem. Eur. J.* **12**, 1889 (2006).
 44. L. Alloatt, R. Palmer, S. Diebold, K. P. Pahl, B. Chen, R. Dinu, M. Fournier, J.-M. Fedeli, T. Zwick, W. Freude, C. Koos, and J. Leuthold, *Light. Sci. & Appl.* **3**, e173 (2014). Number: 5 Publisher: Nature Publishing Group.